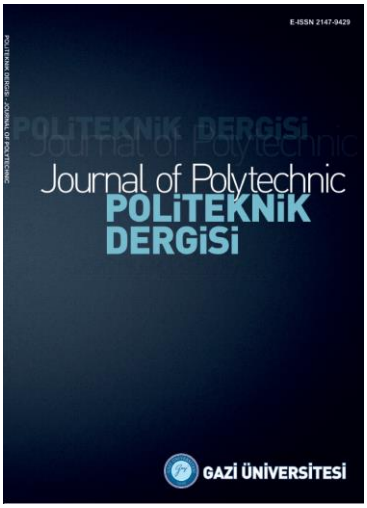


**POLİTEKNİK DERGİSİ**

***JOURNAL of POLYTECHNIC***

ISSN: 1302-0900 (PRINT), ISSN: 2147-9429 (ONLINE)
URL: http://dergipark.org.tr/politeknik



# Investigation of the optical properties of bovine tissues at 635 nm: integrating sphere measurements and monte carlo simulations

## *İnek dokularının 635 nm'deki optik özelliklerinin araştırılması: toplayıcı küre ölçümleri ve monte carlo simülasyonları*

***Yazar(lar) (Author(s))**: Halil ARSLAN[1,2], Abdulrahman ALSHEİKH[2]*

*ORCID[1]: 0000-0001-6176-9719*

*ORCID[2]: 0009-0003-2431-3386*



**To cite to this article**: Arslan H. and Alsheikh A., "Investigation of the Optical Properties Of Bovine Tissues at 635 Nm: İntegrating Sphere Measurements and Monte Carlo Simulations", ***Journal of Polytechnic***, *(*): *, (*).

**Bu makaleye şu şekilde atıfta bulunabilirsiniz:** Arslan H. ve Alsheikh A., "Investigation of the Optical Properties Of Bovine Tissues at 635 Nm: İntegrating Sphere Measurements and Monte Carlo Simulations", ***Politeknik Dergisi***, *(*): *, (*).

**Erişim linki (To link to this article):** http://dergipark.org.tr/politeknik/archive

**DOI:** 10.2339/politeknik.1649712

# Investigation of the Optical Properties of Bovine Tissues at 635 nm: Integrating Sphere Measurements and Monte Carlo Simulations

## *Highlights*

- *Characterization of optical properties of bovine muscle, heart, brain, kidney, and fat tissues.*
- *Application of single integrating sphere and IAD algorithm for optical parameter estimation.*
- *Tissue-dependent variations in absorption and reduced scattering coefficients.*

## *Graphical Abstract*

*Optical properties of bovine muscle, heart, brain, kidney, and fat tissues were experimentally characterized using a single integrating sphere and inverse adding-doubling algorithm.*

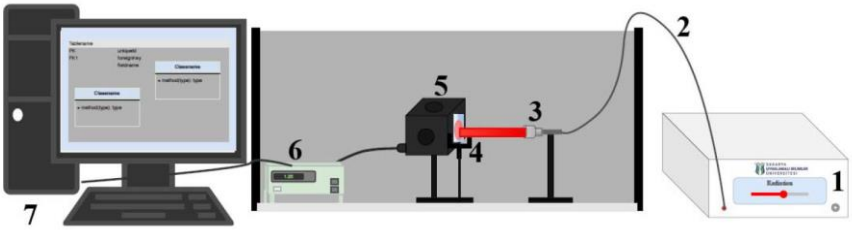


**Figure.** Schematic illustration of the experimental setup

## *Aim*

*The aim of this study is to determine the optical properties of various bovine tissues using integrating sphere system.*

## *Design & Methodology*

*An integrating sphere system combined with the inverse adding-doubling method was used for characterization.*

## *Originality*

*This study compares the optical properties of different types of bovine tissues.*

## *Findings*

*The optical properties showed remarkable variations among muscle, heart, brain, kidney, and fat tissues.*

## *Conclusion*

*The results provide reliable parameters that can support biomedical applications and tissue modeling studies.*

## *Declaration of Ethical Standards*

*The author(s) of this article declare that the materials and methods used in this study do not require ethical committee permission and/or legal-special permission.*

# Investigation of the Optical Properties of Bovine Tissues at 635 nm: Integrating Sphere Measurements and Monte Carlo Simulations

*Araştırma Makalesi / Research Article*

**Halil ARSLAN[1,2*], Abdulrahman ALSHEIKH[2]**

[1]Electrical and Electronics Engineering Department, Sakarya University of Applied Sciences, Sakarya, Turkey
[2]Biomedical Technologies Application and Research Center (Biyotam), Sakarya University of Applied Sciences, Sakarya, Turkey

(Geliş/Received : 03.03.2025 ; Kabul/Accepted : 11.08.2025 ; Erken Görünüm/Early View : 28.09.2025 )

**ABSTRACT**

Understanding the optical properties of biological tissues is essential for optimizing light-based medical applications such as phototherapy, laser surgery, and biomedical imaging. In this study, the absorption coefficient ($\mu_a$) and reduced scattering coefficient ($\mu_s'$) of bovine muscle, heart, brain, kidney and fat tissues were determined at 635 nm using an integrating sphere system and Inverse Adding-Doubling (IAD) method. The experimental results were then used as input parameters for Monte Carlo (MCML) simulations to model light propagation and determine fluence rate distributions within the tissue models. The results demonstrated significant variations in optical properties across different types of tissue, with brain and fat tissues exhibiting lower penetration depths due to higher scattering coefficients. The findings align with previous literature while providing a more comprehensive evaluation through the integration of experimental and computational approaches.

**Keywords: Tissue, Integrating Sphere System, IAD, Monte Carlo Simulation.**

# İnek Dokularının 635 nm'deki Optik Özelliklerinin Araştırılması: Toplayıcı Küre Ölçümleri ve Monte Carlo Simülasyonları

**ÖZ**

Biyolojik dokuların optik özelliklerinin bilinmesi, fototerapi, lazer cerrahisi ve biyomedikal görüntüleme gibi ışık tabanlı tıbbi uygulamaları optimize etmek için önemlidir. Bu çalışmada, inekten alınan kas, kalp, beyin, böbrek ve yağ dokularının 635 nm'deki soğurma katsayısı ($\mu_a$) ve indirgenmiş saçılma katsayısı ($\mu_s'$) değerleri, entegre küre sistemi ve Ters Ekleme-Katlama (IAD) yöntemi kullanılarak belirlendi. Deneysel sonuçlar, ışığın doku modelleri içindeki yayılımını modellemek ve optik doz dağılımlarını belirlemek için MCML simülasyonlarında giriş parametreleri olarak kullanıldı. Farklı doku türlerinin optik özelliklerinin farklı olduğu, beyin ve yağ dokularının görece yüksek saçılma katsayıları nedeniyle daha düşük penetrasyon derinlikleri görülmüştür. Deney ve Monte Carlo simülasyonlarının birlikte kullanıldığı bu çalışmada literatürle uyumlu sonuçlar elde edilmiştir.

**Anahtar Kelimeler: Doku, Toplayıcı Küre Sistemi, IAD, Monte Carlo Simülasyonu.**



## 1. INTRODUCTION

The use of light in medical diagnosis and therapy has gained important attention because of its non-invasive nature and effectiveness in various applications. Light-based techniques, such as laser therapy and optical imaging, are widely used for detecting and treating medical conditions across multiple fields, including oncology, dermatology, and cosmetology. These techniques rely on light-tissue interaction, where absorption and scattering play a fundamental role to determine the behavior of light within the tissue.

For example, when light penetrates skin tissue, it undergoes complex interactions, primarily through absorption and scattering. Absorption occurs due to the presence of key chromophores, like melanin and hemoglobin, while scattering results from cellular structures and other tissue components [1]. The extent of these interactions depends mainly on the wavelength of the incident light and the structural composition of the tissue. Understanding the propagation of laser light through biological tissues is essential for optimizing both diagnostic accuracy and therapeutic efficacy [2]. Accurate modeling of light-tissue interactions allows for improved design and application of optical techniques in medical and cosmetic fields.

To predict the reflection, transmission, and absorption of light within tissues, various theoretical and computational models have been developed. The reliability of these models depends on the precise characterization of the tissue's optical parameters, such as the absorption coefficient and scattering coefficient [3]. These parameters are derived by converting

*Sorumlu Yazar (Corresponding Author)
e-Posta : harslan@subu.edu.tr

observable quantities, such as diffuse reflectance and transmittance, into physical values that describe how light propagates through tissue [4]. Comprehensive knowledge about the tissue optical properties is crucial for enhancing the performance of both diagnostic and therapeutic systems.

The conversion process relies on specific theories of light transport in biological tissues, which describe how light interacts with and propagates through complex biological structures. This propagation is typically characterized by several key optical parameters, including the refractive index ($n$), absorption coefficient ($\mu_a$), scattering coefficient ($\mu_s$) and anisotropy factor ($g$) [5]. The refractive index determines the speed of light within the tissue relative to its speed in a vacuum, while the absorption coefficient quantifies how much light energy is absorbed per unit distance inside the tissue. The scattering coefficient describes the frequency of light scattering events as it travels through the tissue. In addition, anisotropy factor indicates the preferred direction of scattering. Accurate determination of these parameters is essential for modeling light behavior in biological tissues and improving the precision of optical diagnostic and therapeutic applications.

Various experimental techniques were employed to determine the optical parameters of different biological tissues. Among these, the Single or Double Integrating Sphere system is one of the commonly used methods [6, 7]. The sphere system is a hollow spherical structure with a highly reflective inner surface, which facilitates the uniform distribution of light within the sphere [8]. Using this setup, the total diffuse reflection and diffuse transmittance of tissue samples can be measured, both of which are essential inputs for mathematical models used to calculate optical parameters [9].

The Inverse Adding-Doubling (IAD) method is widely utilized to derive the optical parameters of the tissues using experimentally obtained total reflection and transmittance values [10]. This approach is particularly advantageous due to its accuracy in handling highly scattering media, such as biological tissues. The integrating sphere system was used successfully in many studies to determine the optical properties of various tissue types in vitro across a broad wavelength range, from 630 nm to 1064 nm (see, for example, [11-14]). These measurements are critical for improving the understanding of light-tissue interactions and for enhancing the design of optical diagnostic and therapeutic devices.

Monte Carlo simulations are widely used to estimate light propagation within biological tissues. This method models the expected motion of individual photons, treating them as light particles that follow specific probability density functions for their movement. In other words, Monte Carlo simulations generate detailed maps of light distribution in tissues and offer a flexible and robust approach to modeling light transport [15]. Several software programs are available to simulate radiation interactions with matter, one of which is the code called Monte Carlo Modeling of Light Transport in Multi-Layered Tissues (MCML) [16]. This software allows for the creation of customized material models and provides detailed information on the physical processes affecting photon transport within the material.

Recent studies have emphasized the importance of accurately characterizing the optical properties of biological tissues to improve the efficiency of laser-based biomedical applications. For instance, Shahin et al. investigated the optical behavior of bovine white and grey matter preserved in formalin over a spectral range of 440–1000 nm, using a single integrating sphere system combined with an inverse adding-doubling algorithm [17]. Their results highlighted significant differences between white and grey matter, as well as the influence of storage conditions on optical properties. Complementarily, Hamdy and Mohammed examined the dependence of tissue optical properties on incident infrared laser power. Utilizing an integrating sphere together with the Kubelka-Munk model and COMSOL Multiphysics simulations, they demonstrated the relationship between laser power and variations in scattering and absorption coefficients [18].

In recent years, advances in computational modeling have significantly contributed to the field of tissue optics. GPU-accelerated Monte Carlo simulations have enabled faster and more efficient modeling of photon propagation in heterogeneous media, supporting complex biomedical applications [19]. Additionally, the integration of experimental datasets with Monte Carlo-based diffuse optical spectroscopy has facilitated more accurate three-dimensional modeling of tissue optical properties [20]. Complementing these developments, novel frameworks for inverse problem validation have improved the reliability of optical parameter estimation, further strengthening the methodological foundation of simulation-based optical studies [21].

In this study, the absorption and reduced scattering coefficients of various bovine tissues, including muscle, myocardial, brain, kidney, and fat were determined using a 635 nm FDT laser device and a single integrating sphere measurement system. The experimental results were also utilized as input parameters for Monte Carlo simulations to investigate the fluence rate distributions within the tissue models.

## 2. MATERIAL and METHOD

In this study, total diffuse reflection and transmittance values of bovine tissues were measured using a single integrating sphere system. The experimental setup, as described in a prior study [22], is schematically presented in Figure 1.

A 635 nm multimode photodynamic therapy (PDT) laser device operating in continuous mode was employed as the light source. The integrating sphere system employed in this study was operated in accordance with the manufacturer's recommended calibration protocol.

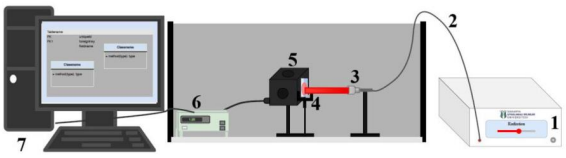


**Figure 1.** Schematic illustration of the experimental setup: (1) PDT laser device, (2) fiber optic cable, (3) collimator, (4) tissue samples, (5) integrating sphere, (6) photodiode amplifier, and (7) computer.

The inner surface of the sphere was coated with a high-reflectivity material, and its reflectance was treated as a constant parameter throughout the measurements. The system was specifically designed to collect and quantify both reflected and transmitted light from the tissue samples, which is critical for the accurate determination of their optical properties.

Fresh bovine tissue samples, including muscle, myocardial, brain, kidney, and fat, were obtained and prepared under controlled conditions. From each tissue type, five samples with varying thicknesses were carefully prepared to ensure consistency and reproducibility. Each sample was cut to a defined thickness to minimize variability and ensure uniformity across measurements. The samples were immediately measured to preserve their optical properties and prevent tissue degradation. Previous studies, such as [22], have demonstrated that the optical properties of tissues undergo significant changes during processes like drying or coagulation.

The laser beam was directed perpendicularly onto the tissue samples placed within the integrating sphere system. For each tissue type, total diffuse reflectance and diffuse transmittance values were recorded. To minimize experimental errors, multiple measurements were carried out for each sample, and the average values were calculated for further analysis.

To ensure statistical reliability, measurements were repeated independently on all five samples for each tissue type. This approach enabled the calculation of mean values and standard deviations, which were subsequently used to reflect experimental uncertainty in the derived optical parameters, including the absorption and reduced scattering coefficients.

The measurement data, including diffuse reflectance, transmittance, sample thickness, and geometrical and optical properties of the integrating sphere, were compiled into input files. These input files were processed using IAD method, a well-established computational technique for obtaining optical parameters from experimental data. Through iterative calculations, the absorption and reduced scattering coefficients of each tissue sample were derived. The uncertainty values associated with the calculated optical parameters were estimated based on the standard deviation of multiple independent measurements performed for each tissue type.

To simulate light propagation within the tissue models, the MCML program was used. This code is a steady-state Monte Carlo simulation tool designed to model photon transport through multilayered, turbid media. It assumes an infinitely narrow photon beam incident perpendicularly on the tissue surface. The simulation procedure, including the definition of tissue geometry and optical parameter specification, and data acquisition steps, is schematically represented in Figure 2.

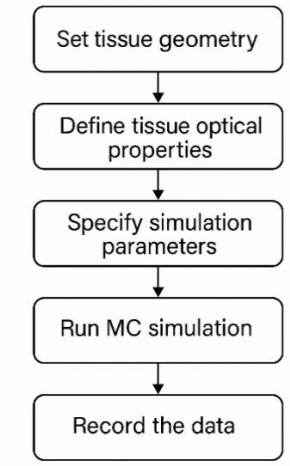


**Figure 2.** Flowchart illustrating the MC simulation steps for light propagation in tissue models.

Each layer within the model was initially defined by setting the tissue geometry as a single-layer, homogeneous structure in the shape of a cylindrical disk with 1 mm thickness, representing the physical structure of the samples. Subsequently, the optical properties of each tissue, including the absorption coefficient ($\mu_a$), scattering coefficient ($\mu_s$), anisotropy factor (g), and refractive index (n), were assigned. The experimentally obtained optical parameters for muscle, myocardial, brain, kidney, and fat tissues were used as input for the MCML simulations. Additionally, refractive index and anisotropy factor values for each tissue type were sourced from the literature [4, 14] and incorporated into the simulation.

After defining the tissue geometry and optical properties, the simulation parameters were specified. Monte Carlo simulations were performed using 1,000,000 photons at a wavelength of 635 nm to ensure statistical accuracy and minimize noise in the fluence rate distributions. Following the simulation runs, the fluence rate distributions within the tissue models were recorded, providing a detailed map of photon propagation and absorption across different tissue environments. The resulting data offered valuable insights into light-tissue interactions, enabling a comprehensive analysis of photon transport and optical dose distribution in various bovine tissues.

## 3. RESULTS AND DISCUSSION

In this study, $\mu_a$ and $\mu_s'$ of five different bovine tissues (brain, fat, kidney, muscle, and heart) were determined at 635 nm using a single integrating sphere measurement system and analyzed through IAD method. The experimentally obtained values are given in Table 1 together with previously reported data at similar wavelengths.

The absorption coefficient of brain tissue was measured as 0.028 ± 0.008 $mm^{-1}$, which is higher than the value of 0.015 $mm^{-1}$ exist in the literature for 633 nm [23]. This discrepancy may be attributed to differences in tissue preparation methods, hydration levels, or anatomical variations between samples. Moreover, the reduced scattering coefficient determined in this study (4.04 ± 0.96 $mm^{-1}$) is found to be lower than the literature value (6.10 $mm^{-1}$), indicating that light scattering in brain tissue is less pronounced under our experimental conditions. This reduction may result from variations in cell density or lipid content, both of which can influence the scattering behavior of neural tissues.

Furthermore, the absorption coefficient of muscle tissue was determined to be 0.29 ± 0.06 $mm^{-1}$, which is higher than the value of 0.18 $mm^{-1}$ previously found for 650 nm [23]. This increase may be attributed to higher myoglobin or water content, both of which are strong absorbers at wavelengths near 635 nm. In contrast, the reduced scattering coefficient (0.56 ± 0.08 $mm^{-1}$) is slightly lower than the literature value (0.72 $mm^{-1}$). This minor discrepancy might be due to differences in muscle fiber orientation and the degree of tissue hydration.

Moreover, measured absorption coefficient for the heart tissue (0.21 ± 0.05 $mm^{-1}$) is also higher than the literature value (0.10 $mm^{-1}$) [23]. This substantial difference suggests that myocardial tissue may exhibit considerable variability in chromophore concentrations, particularly hemoglobin. However, the reduced scattering coefficient (1.49 ± 0.03 $mm^{-1}$) closely matches the previously reported value (1.5 $mm^{-1}$), indicating similar structural properties despite variations in absorption. This agreement in scattering coefficients supports the assumption that cardiac muscle maintains a consistent microarchitecture across different samples.

**Table 1.** Optical properties of various bovine tissues.

| Tissue type | $\mu_a$ ($mm^{-1}$) | $\mu_s'$ ($mm^{-1}$) | Wavelength (nm) | Ref. |
|---|---|---|---|---|
| Brain | 0.015 | 6.10 | 633 | [23] |
| | 0.028 ± 0.008 | 4.04 ± 0.96 | 635 | This study |
| Fat | 0.026 | 1.22 | 633 | [24] |
| | 0.022 ± 0.009 | 1.1 ± 0.15 | 635 | This study |
| Kidney | 0.20 | 0.42 | 633 | [25] |
| | 0.31 ± 0.07 | 0.71 ± 0.09 | 635 | This study |
| Muscle | 0.18 | 0.72 | 650 | [23] |
| | 0.29 ± 0.06 | 0.56 ± 0.08 | 635 | This study |
| Heart | 0.10 | 1.5 | 650 | [23] |
| | 0.21 ± 0.05 | 1.49 ± 0.03 | 635 | This study |

For fat tissue, the absorption coefficient (0.022 ± 0.009 $mm^{-1}$) aligns closely with the literature value (0.026 $mm^{-1}$) at 633 nm [24], which is within the experimental uncertainty range. The reduced scattering coefficient (1.10 $mm^{-1}$) also exhibits good agreement with the previously reported value (1.22 $mm^{-1}$). This consistency suggests that fatty tissues exhibit stable optical properties across small wavelength variations, largely due to the homogeneity of lipid structures that dominate their composition.

In addition, kidney tissue displayed a higher absorption coefficient (0.31 ± 0.07 $mm^{-1}$) compared to the literature value (0.20 $mm^{-1}$) [25]. This difference may stem from biological variability or differences in the vascular content of the samples, as kidney tissues are highly perfused organs. The reduced scattering coefficient (0.71 ± 0.09 $mm^{-1}$) is also higher than the literature value (0.42 $mm^{-1}$), suggesting increased microstructural complexity or greater cellular heterogeneity in the tested samples.

The relationship between the optical properties obtained in this study and those reported in the literature was evaluated through linear regression analysis (Figure 3). Different tissues are indicated by distinct markers and colors, and the dashed lines represent the linear regression fits. For the absorption coefficient ($\mu_a$), the regression yielded a slope of 1.24 indicating a strong positive correlation and a slight systematic deviation. Similarly, for the reduced scattering coefficient ($\mu_s'$), a slope of 0.85 were obtained. These results demonstrate a consistent trend with the data obtained by different groups, although minor deviations are observed, which can be attributed to differences in sample preparation, tissue heterogeneity, and measurement conditions. The high degree of correlation supports the reliability and validity of the experimental methodology employed in this study.

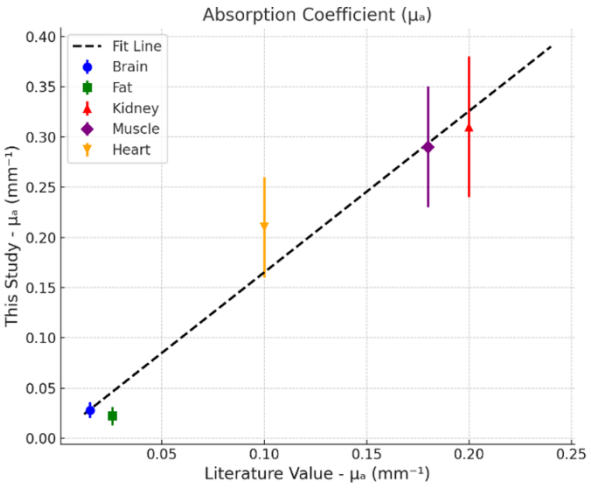


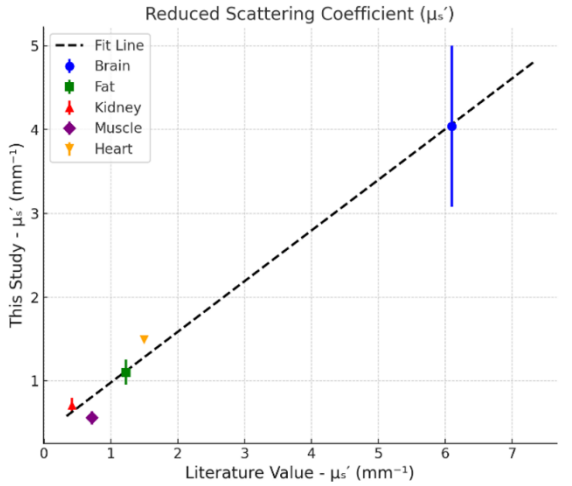


**Figure 3.** Linear regression analysis comparing the experimental absorption ($\mu_a$) and reduced scattering ($\mu_s'$) coefficients with corresponding values reported in the literature.

Figure 4 presents the two-dimensional distribution of optical power density for heart, brain, muscle, kidney, and fat tissue models at 635 nm, obtained using the MCML simulation code. These distributions provide insight into how light propagates and interacts within each tissue type, highlighting variations in absorption and scattering characteristics.

In each tissue model, light was introduced as a point source of collimated photons at coordinates r = 0 and z = 0. The optical power density distributions, illustrated in the figure, are presented on a logarithmic scale to provide a clearer visualization of variations across different tissue types. Because of the differences in the optical parameters, specifically the absorption and the reduced scattering coefficients, distribution of optical power density varied significantly among the tissue models. The depth that light can reach within the tissue is directly influenced by these parameters, resulting in distinct propagation patterns for each tissue type.

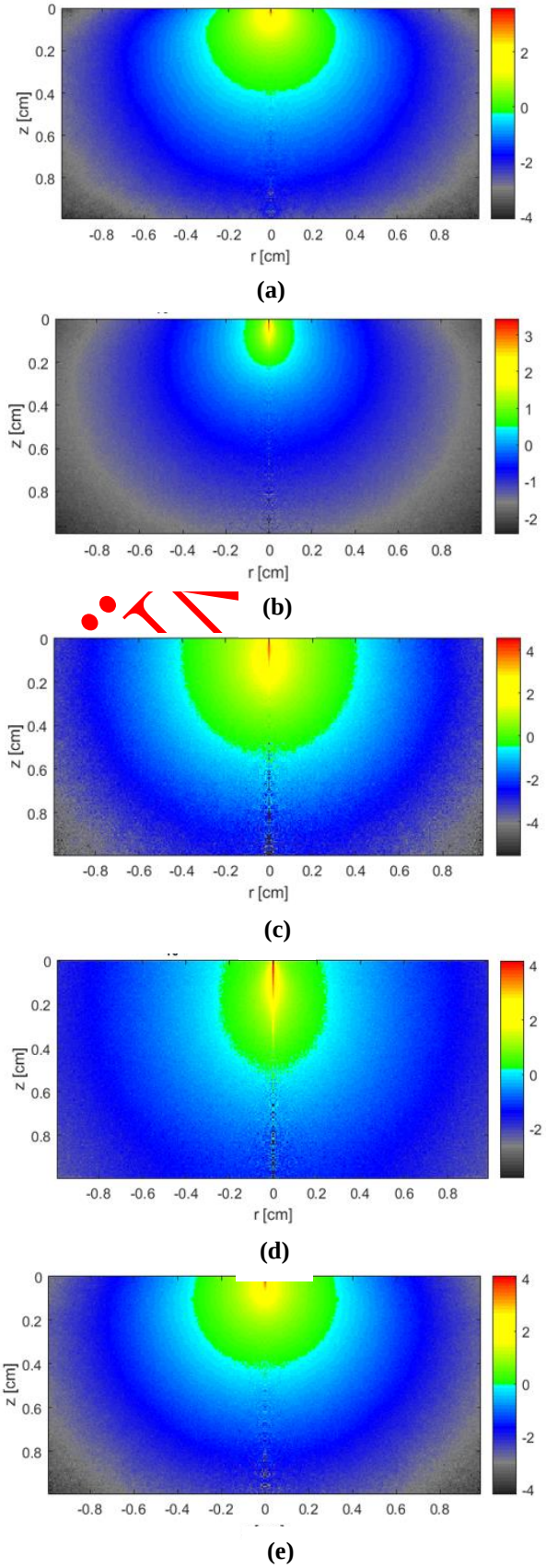


**Figure 4.** Two-dimensional optical power density of 633 nm light in brain (a), fat (b), kidney (c), muscle (d) and heart (e) tissue models.

Among the tissue models, the brain and fat tissues (Figure 4a and Figure 4b) exhibit more limited penetration depths compared to the other samples although they have relatively lower absorption coefficients. This reduced penetration is primarily attributed to the higher reduced scattering coefficients of such tissues, which increase the likelihood of photon deflection as the light propagates. As a result, photon trajectories become more randomized, reducing the number of photons that can penetrate deeper layers and leading to a steeper decline in optical power density with increasing depth.

Additionally, the increased scattering causes a higher probability of photon absorption due to the prolonged photon path length within the tissue. This phenomenon is consistent with established light-tissue interaction principles, where tissues with elevated scattering coefficients exhibit lower optical penetration due to increased photon scattering and absorption events. The observed differences in optical power density distributions underscore the critical role of tissue-specific optical parameters in determining light propagation and energy deposition within biological tissues.

## 4. CONCLUSION

The optical properties of various bovine tissues, including muscle, myocardial, brain, kidney, and fat, were systematically investigated in this study for the wavelength of 635 nm. Using the single integrating sphere system, the total transmittance and reflectance of each tissue type were measured. The absorption and reduced scattering coefficients were then determined through the IAD method. Additionally, Monte Carlo simulations were utilized using the MCML code to model the optical power density distribution within each tissue type.

The results indicate that the optical parameters vary significantly across different tissue types, leading to distinct light penetration behaviors. Among the tissues analyzed, brain and fat exhibited the lowest penetration depths, primarily due to their higher reduced scattering coefficients. These findings align with existing literature, further validating the accuracy of the experimental and computational approaches employed in this study.

The integration of experimental measurements with Monte Carlo simulations provides a comprehensive understanding of light-tissue interactions, offering valuable insights for biomedical applications. Accurate knowledge of tissue-specific optical properties is crucial for optimizing phototherapy techniques, medical imaging, and laser-based diagnostic procedures. Future work may extend these methods to a broader range of tissue types and wavelengths to enhance the precision of light-tissue interaction models and support the development of advanced optical medical technologies.

## DECLARATION OF ETHICAL STANDARDS

The authors declare that the materials and methods used in this study did not require ethics committee approval and/or any legal or special permission.

## AUTHORS' CONTRIBUTIONS

**Halil ARSLAN:** Performed the analysis of the results and wrote the manuscript.

**Abdulrahman ALSHEIKH:** Conducted the experiments and simulation studies.

## CONFLICT OF INTEREST

The authors declare that there is no conflict of interest regarding this study.

## REFERENCES


[1] Fodor, L., Ullmann, Y., & Elman, M. ***Aesthetic applications of intense pulsed light*** (pp. 11-20). London: Springer, (2011).

[2] Ash, C., Dubec, M., Donne, K., & Bashford, T. "Effect of wavelength and beam width on penetration in light-tissue interaction using computational methods", ***Lasers in Medical Science***, 32, 1909-1918, (2017).

[3] Tuchin, V. V. "Tissue optics and photonics: light-tissue interaction", ***Journal of Biomedical Photonics & Engineering***, 1(2), 98-134, (2015).

[4] Jacques, S. L. "Optical properties of biological tissues: a review", ***Physics in Medicine & Biology***, 58(11), R37, (2013).

[5] Cheong, W. F., Prahl, S. A., & Welch, A. J. "A review of the optical properties of biological tissues", ***IEEE Journal of Quantum Electronics***, 26(12), 2166–2185, (1990).

[6] Welch, A. J., & Van Gemert, M. J. (Eds.) ***Optical-thermal response of laser-irradiated tissue*** (Vol. 2) New York: Springer, (2011).

[7] Hamdy, O., Fathy, M., Al-Saeed, T. A., El-Azab, J., & Solouma, N. H. "Estimation of optical parameters and fluence rate distribution in biological tissues via a single integrating sphere optical setup", ***Optik***, 140, 1004-1009, (2017).

[8] Kienle, A., Lilge, L., Patterson, M. S., Hibst, R., Steiner, R., & Wilson, B. C. "Spatially resolved absolute diffuse reflectance measurements for noninvasive determination of the optical scattering and absorption coefficients of biological tissue", ***Applied Optics***, 35(13), 2304-2314, (1996).

[9] Prahl, S. A., van Gemert, M. J., & Welch, A. J. "Determining the optical properties of turbid media by using the adding–doubling method", ***Applied Optics***, 32(4), 559-568, (1993).

[10] De Vries, G., Beek, J. F., Lucassen, G. W., & Van Gemert, M. J. C. "The effect of light losses in double integrating spheres on optical properties estimation", ***IEEE Journal of Selected Topics in Quantum Electronics***, 5(4), 944-947, (1999).

[11] Pickering, J. W., Prahl, S. A., Van Wieringen, N., Beek, J. F., Sterenborg, H. J., & Van Gemert, M. J. "Double-integrating-sphere system for measuring the optical properties of tissue", ***Applied Optics***, 32(4), 399-410, (1993).

[12] Beek, J. F., Blokland, P., Posthumus, P., Aalders, M., Pickering, J. W., Sterenborg, H. J. C. M., & Van Gemert, M. J. C. "In vitro double-integrating-sphere optical properties of tissues between 630 and 1064 nm", ***Physics in Medicine & Biology***, 42(11), 2255, (1997).

[13] Pehlivanöz, B., & Arslan, H. "Estimation of optical parameters of chicken liver tissue via single integrating-sphere system", ***Medical Technologies National Congress*** (TIPTEKNO) pp. 1-3, (2018).

[14] Martins, I. S., Silva, H. F., Lazareva, E. N., Chernomyrdin, N. V., Zaytsev, K. I., Oliveira, L. M., & Tuchin, V. V. "Measurement of tissue optical properties in a wide spectral range: a review", ***Biomedical Optics Express***, 14(1), 249-298, (2022).

[15] Krasnikov, I., Seteikin, A., & Roth, B. "Advances in the simulation of light–tissue interactions in biomedical engineering", ***Biomedical Engineering Letters***, 9, 327-337, (2019).

[16] Wang, L., Jacques, S. L., & Zheng, L. "MCML—Monte Carlo modeling of light transport in multi-layered tissues", ***Computer Methods and Programs in Biomedicine***, 47(2), 131-146, (1995).

[17] Shahin, A., Bachir, W. & El-Daher, M. S. "Optical investigation of bovine grey and white matters in visible and near-infrared ranges", ***Polish Journal of Medical Physics and Engineering***, 27(1), 99-107, (2021).

[18] Hamdy, O. & Mohammed, H. S. "Variations in tissue optical parameters with the incident power of an infrared laser", ***PLoS One***, 17(1), 0263164, (2022).

[19] Ren, N., Liang, J., Qu, X., Li, J., Lu, B., & Tian, J. "GPU-based Monte Carlo simulation for light propagation in complex heterogeneous tissues", ***Optics Express***, 18(7), 6811–6823, (2010).

[20] Moradi, M., & Chen, Y. "Monte Carlo simulation of diffuse optical spectroscopy for 3D modeling of dental tissues", ***Sensors***, 23(11), 5118, (2023).

[21] Adler, T. J., Nölke, J. H., Reinke, A., Tizabi, M. D., Gruber, S., Trofimova, D., ... & Maier-Hein, L. "Application-driven validation of posteriors in inverse problems", ***Medical Image Analysis***, 101, 103474, (2025).

[22] Arslan, H., & Pehlivanoz, B. "Effect of purification, dehydration, and coagulation processes on the optical parameters of biological tissues", ***Chinese Optics Letters***, 19(1), 011701, (2021).

[23] Lanka, P., Francis, K. J., Kruit, H., Farina, A., Cubeddu, R., Sekar, S. K. V., ... & Pifferi, A. "Optical signatures of radiofrequency ablation in biological tissues", ***Scientific Reports***, 11(1), 6579, (2021).

[24] Kienle, A., Lilge, L., Patterson, M. S., Hibst, R., Steiner, R., & Wilson, B. C. "Spatially resolved absolute diffuse reflectance measurements for noninvasive determination of the optical scattering and absorption coefficients of biological tissue", ***Applied Optics***, 35(13), 2304-2314, (1996).

[25] Botelho, A. R., Silva, H. F., Martins, I. S., Carneiro, I. C., Carvalho, S. D., Henrique, R. M., ... & Oliveira, L. M. "Fast calculation of spectral optical properties and pigment content detection in human normal and pathological kidney", ***Spectrochimica Acta Part A: Molecular and Biomolecular Spectroscopy***, 286, 122002, (2023).